

The unstable fate of the planet orbiting the A-star in the HD 131399 triple stellar system

Dimitri Veras^{1*}, Alexander J. Mustill², Boris T. Gänsicke¹

¹*Department of Physics, University of Warwick, Coventry CV4 7AL, UK*

²*Lund Observatory, Department of Astronomy and Theoretical Physics, Lund University, Box 43, SE-221 00 Lund, Sweden*

31 October 2016

ABSTRACT

Validated planet candidates need not lie on long-term stable orbits, and instability triggered by post-main-sequence stellar evolution can generate architectures which transport rocky material to white dwarfs, polluting them. The giant planet HD 131399Ab orbits its parent A star at a projected separation of about 50-100 au. The host star, HD131399A, is part of a hierarchical triple with HD131399BC being a close binary separated by a few hundred au from the A star. Here, we determine the fate of this system, and find that (i) stability along the main sequence is achieved only for a favourable choice of parameters within the errors, and (ii) even for this choice, in almost every instance the planet is ejected during the transition between the giant branch and white dwarf phases of HD 131399A. This result provides an example of both how the free-floating planet population may be enhanced by similar systems, and how instability can manifest in the polluted white dwarf progenitor population.

Key words: minor planets, asteroids: general – stars: white dwarfs – methods: numerical – celestial mechanics – planet and satellites: dynamical evolution and stability – protoplanetary discs

1 INTRODUCTION

Direct imaging provides an invaluable window into the outer reaches of planetary systems (Bryan et al. 2016; Clanton & Gaudi 2016a; Durkan et al. 2016; Reggiani et al. 2016). Beyond about 5 au, the indirect planet-detection techniques of Doppler radial velocity and transit photometry are effectively blind. Nevertheless, our Solar system and the HR 8799 system (Marois et al. 2008, 2010) demonstrate that many giant planets beyond 5 au can co-exist, as well as rocky minor planets, such as Pluto, moons like Triton, and vast belts such as the Kuiper Belt and scattered disc.

This material in the outer reaches of planetary systems largely survives the giant branch evolution of their parent stars (Veras 2016a), even amidst dynamical excitation from the presence of a binary stellar companion (Bonsor & Veras 2015; Hamers & Portegies Zwart 2016a; Petrovich & Muñoz 2016) or a distant Planet Nine analogue (Veras 2016b). The directly imaged $7M_{\text{Jup}}$ planet orbiting the white dwarf WD 0806-661 at a distance of approximately 2500 au (Luhman et al. 2011) provides a perhaps extreme example of the survivability of some planets orbiting evolved stars. White dwarfs in wide binaries have in fact been used to

help constrain planet formation in the presence of a stellar companion (Zuckerman 2014).

The direct imaging discovery of a $4M_{\text{Jup}}$ planet in the HD 131399 triple star system (Wagner et al. 2016) – where the planet orbits its single parent star at a distance of about 50-100 au – provides a helpful opportunity to study long-term stability across multiple phases of stellar evolution in a dynamically complex environment. The planet-host, HD 131399A, is an A-star (with a mass of about $1.8M_{\odot}$), which represents the progenitor stellar type of the white dwarfs most commonly observed today (Tremblay et al. 2016). The two companion stars (HD 131399B and HD 131399C) form a tight binary whose barycentre orbits HD 131399A at a distance of just a few hundred au (see Tables 1-2). The wide separation of the planet allows for ensembles of full-lifetime simulations to be carried out, and the tightness of the HD 131399B and HD 131399C mutual orbit allows them to be treated as a single object (see e.g. right panel of Fig. S3 of Wagner et al. 2016).

This paper explores the fate of HD 131399Ab. We first describe in Section 2 why studying the long-term evolution of planetary systems is so important, before setting up the simulations in section 3, presenting the results in section 4, and concluding in section 5.

* E-mail: d.veras@warwick.ac.uk

2 IMPORTANCE OF DETERMINING FATE

The fates of planetary systems provide unique chemical and dynamical constraints that directly link to their formation.

Chemically, within the atmospheres of white dwarfs up to 20 different metals from planetary debris have now been measured (Gänsicke et al. 2012; Jura & Young 2014; Xu et al. 2014; Melis & Dufour 2016; Wilson et al. 2016). This debris predominately arises from tidal break-up (Debes et al. 2012; Veras et al. 2014a, 2015a, 2016a) of progenitor asteroids which have compositions that could be mapped to particular Solar system asteroid families (e.g. Fig. 7 of Gänsicke et al. 2012 and Fig. 10 of Wilson et al. 2015). In about 40 cases, discs of this debris have been detected (Zuckerman & Becklin 1987; Farihi 2016). All of the discs are dusty, and gaseous components have been detected in some (Gänsicke et al. 2006; Manser et al. 2016a). The discs themselves are protean, demonstrating a remarkable variability (Wilson et al. 2014; Xu & Jura 2014; Manser et al. 2016b), and potential eccentricity (Dennihey et al. 2016), and all orbit white dwarfs which are chemically polluted. The likely disruption of an asteroid orbiting WD 1145+017 (Vanderburg et al. 2015; Gänsicke et al. 2016; Gary et al. 2016; Gurri et al. 2016; Rappaport et al. 2016; Veras et al. 2016a) is accompanied by both chemical signatures in circumstellar gas (Xu et al. 2016) and chemical pollution within the white dwarf itself.

Dynamically, snapshots of planetary systems at different ages help piece together their life cycles. Old main sequence systems (e.g. Campante et al. 2015), dust and planets around giant branch stars (Bonsor et al. 2014; Trifonov et al. 2015; Lillo-Box et al. 2016; Wittenmyer et al. 2016), and polluted white dwarfs at a variety of cooling ages (Koester et al. 2014; Hollands et al. 2016) all provide necessary constraints. Main-sequence planetary studies have now begun to utilise white dwarf atmosphere chemical signatures in their planetary formation models (Carter-Bond et al. 2012; Morlok et al. 2014; Bergin et al. 2015; Ramírez et al. 2015; Mordasini et al. 2016; Spina et al. 2016), and future missions such as *PLATO* will further enable comparisons with well-constrained stellar ages (Veras et al. 2015b). Full-lifetime simulations incorporating all of the necessary physics (Fig. 2 of Veras 2016a) have yet to be achieved, although more modest attempts have succeeded in modelling for multiple Gyr the mutual interactions amongst planets (Veras & Gänsicke 2015; Veras et al. 2016b,c), and planets and asteroids (Mustill et al. 2016a). These types of simulations also help determine the viability of some post-main-sequence observations by testing for past stability (Mustill et al. 2013; Portegies Zwart 2013).

One of the most common outcomes of instability in these simulations is ejection, a process that contributes to the free-floating planet population. The striking result that there might exist up to two giant planet free floaters for each Milky Way main sequence star (Sumi et al. 2011) has yet to be explained by theory (Veras & Raymond 2012; Forgan et al. 2015; Wang et al. 2015; Smullen et al. 2016; Sutherland & Fabrycky 2016) and is mitigated by the possibility that a fraction of the purported free-floaters are in

Table 1. Spectral types and masses of the components of the HD 131399 system. All data is reproduced from Wagner et al. (2016).

Component	Ab	A	B	C
Spectral Type	–	A	G	K
Mass	$4 \pm 1 M_{\text{Jup}}$	$1.82 M_{\odot}$	$0.96 M_{\odot}$	$0.60 M_{\odot}$

Table 2. Orbital parameters from the orbit of HD 131399A and HD 131399Ab (*top row*) and the orbit of the barycentre of HD 131399A and HD 131399Ab and the barycentre of HD 131399B and HD 131399C (*bottom row*). a , e and i refer to the semimajor axis, eccentricity and inclination with respect to the plane of the sky. Recall that mutual inclination is defined with respect to both inclination and longitude of ascending node, meaning mutual inclinations generally differ from those assumed by simply looking at the values of i here. All data is reproduced from Wagner et al. (2016).

a_{pl} 82^{+23}_{-27} au	e_{pl} 0.35 ± 0.25	i_{pl} 40^{+80}_{-20} degrees
a_{bin} 270 – 390 au	e_{bin} 0.1 – 0.3	i_{bin} 30 – 70 degrees

fact wide-orbit planets (Clanton & Gaudi 2016b)¹. In any case, mapping ejection prospects with architecture and time over different phases of stellar evolution (Veras et al. 2011; Veras & Tout 2012; Mustill et al. 2014; Veras et al. 2014b; Kostov et al. 2016) can also be explored with the HD 131399 system.

3 SYSTEM SETUP

3.1 Observational constraints

HD 131399 is a triple star system with one planet (HD 131399Ab) orbiting one of the stars (HD 131399A), with the other two stars (HD 131399B and HD 131399C) forming a close binary (Wagner et al. 2016). The masses and spectral types of all four objects are given in Table 1.

Because the system components have been directly imaged, the observables are projected separations, rather than semimajor axes. The large separations imply that years or decades of observations would be necessary to better constrain orbital properties. Fortunately, Wagner et al. (2016) partly accomplished this task by also utilising astrometric data dating back to 1897 (Gill 1897). The result is the orbital parameters given in Table 2. No orbital parameters were estimated for the mutual orbit of HD 131399B and HD 131399C, although Wagner et al. (2016) reports that the difference in their projected separations from HD 131399A is only about 7 au.

¹ Nevertheless the true fraction of giant planet free floaters – perhaps closer to one per main sequence star – remains high relative to predicted occurrence rates from other exoplanet detection techniques.

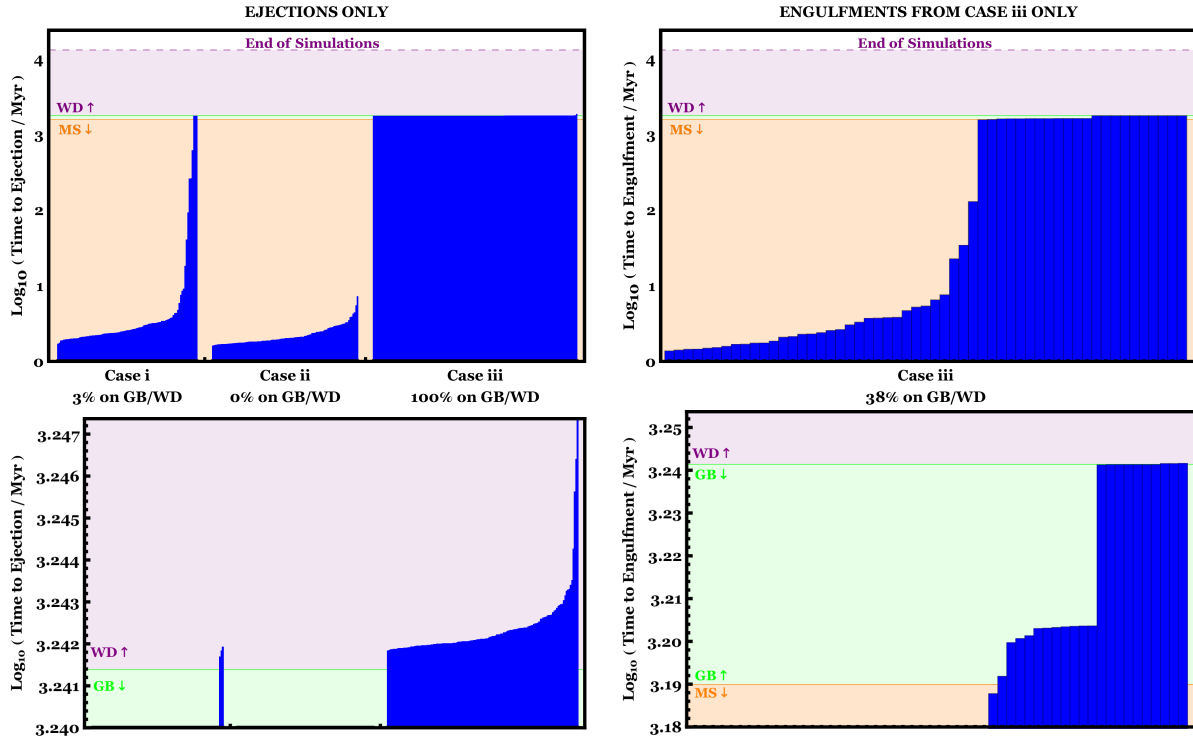


Figure 1. Sorted ejection times (*left-hand panels*) and engulfment times (*right-hand panels*) by case (*case i*: nominal parameter choice; *case ii*: precarious parameter choice; *case iii*: guarded parameter choice - see Sec. 3.3.1.) for the planet HD 131399Ab. The bottom panels are zoomed-in versions of the top panels. Each individual bar represents a single simulation, and time zero corresponds to the currently measured configuration, which is thought to be about 16 Myr old (Wagner et al. 2016). The *x*-axes give the case numbers as well as the fraction of ejections and engulfments that occurred on either the giant branch or white dwarf phase of HD 131399A. Different stellar phases are indicated by shaded regions: orange for main sequence, green for giant branch, and purple for white dwarf. The purple dashed line indicates the ending time of the simulations. Instability occurs in almost every simulation, and nearly-exclusively on the main sequence or during the transition between the giant branch and white dwarf phases, depending on the parameters adopted. In the bottom-right panel, engulfments occur predominantly at the tips of the red giant and asymptotic giant branch phases of HD 131399A.

3.2 Our model

This close proximity of the two non-planet host stars allow us to treat them as a single body with a combined mass of $1.56M_{\odot}$ but with a main sequence lifetime befitting the more massive star (HD 131399B; $0.96M_{\odot}$). We can quantify the goodness of this approximation by considering equation 10 of Hamers & Portegies Zwart (2016b), which represents the ratio of Lidov-Kozai timescales of different orbits in this system. Assume orbit #1 denotes the orbit of HD 131399Ab around HD 131399A, orbit #2 denotes the mutual orbit of HD 131399B and HD 131399C, and orbit #3 denotes the widest orbit, containing both orbits #1 and #2. Then when the equation is applied to the orbit pairs (1,3) and (2,3), for nominal parameters (Table 2) and assuming a semimajor axis of 7.5 au for orbit #2, then the ratio is about $0.03 \ll 1$. Hence, at least from a secular dynamics perspective, the binarity of stars HD 131399B and HD 131399C can be neglected.

If one assumes that HD 131399B has Solar metallicity, then the SSE stellar evolution code (Hurley et al. 2000) predicts a main sequence lifetime of about 12.8 Gyr. In contrast, the main sequence lifetime of the $1.82M_{\odot}$ star HD 131399A is about just 1.5 Gyr, with a shorter giant branch lifetime of 0.2 Gyr.

Therefore, we executed integrations with three bodies

(HD 131399A, HD 131399Ab and the approximated outer stellar companion) for 12.8 Gyr, treating the outer companion as a main sequence star throughout while evolving HD 131399A through the main sequence, giant branch and white dwarf phases of evolution.

3.3 Numerical code

We performed the simulations by using a RADAU-based integrator within the *Mercury* suite (Chambers 1999) that interpolates stellar mass and radius changes from *SSE* (Hurley et al. 2000). Full details of this combined, open-source code are provided in Mustill et al. (2016b). The code improves upon the previous incarnation, a Bulirsch-Stoer based integrator, which was used in several previous studies and introduced in Veras et al. (2013). We adopted an accuracy parameter of 10^{-12} .

3.3.1 Initial conditions

We performed a total of 400 simulations, split into three cases (below) based on the error ranges in Wagner et al. (2016). Within each case, we fixed the mass of HD 131399Ab to be $4M_{\text{Jup}}$, and randomly sampled from a uniform distribution (1) the arguments of pericentre, longitudes of ascending node, and mean anomalies of both orbits in Table 2, and

(2) the inclinations across the ranges given in those tables. These values are somewhat constrained by the observations for the binary, but not for the planet. The constraints on the orbit of the planet are too weak to be useful, justifying this naive approach.

(i) **The nominal case; 100 simulations:** Here we adopted the nominal values of semimajor axes and eccentricities that were given in Wagner et al. (2016). These corresponded to $a_{\text{pl}} = 82$ au, $e_{\text{pl}} = 0.35$, $a_{\text{bin}} = 330$ au and $e_{\text{bin}} = 0.2$.

(ii) **The precarious case; 100 simulations:** Here we minimised the difference between the apocentre of the planet orbit and the pericentre of the mutual stellar orbit. These choices corresponded to $a_{\text{pl}} = 105$ au, $e_{\text{pl}} = 0.70$, $a_{\text{bin}} = 270$ au and $e_{\text{bin}} = 0.3$.

(iii) **The guarded case; 200 simulations:** Here we maximised the difference between the apocentre of the planet orbit and the pericentre of the mutual stellar orbit. These choices corresponded to $a_{\text{pl}} = 55$ au, $e_{\text{pl}} = 0.10$, $a_{\text{bin}} = 390$ au and $e_{\text{bin}} = 0.1$.

Because the maximum apocentre of the mutual stellar orbit that we considered was 429 au, we have neglected effects from Galactic tides and stellar flybys across all stellar phases (Veras et al. 2014b) but adopted realistic Hill ellipsoids to model escape (Veras & Evans 2013; Veras et al. 2014c) assuming a circular Galactic orbit at 8 kpc.

Even before running these simulations, one may obtain a rough sense of the expected outcomes on the main sequence only by appealing to existing stability criteria. One well-used criterion is that from equation 1 of Holman & Wiegert (1999), which estimates the critical semimajor axis within which a circumstellar test particle would be come unstable in the presence of a binary stellar companion. This criterion also assumes full coplanarity, and has been shown to not be fully accurate due to limiting sampling resolution (see Marzari & Gallina 2016). Nevertheless, the Holman & Wiegert (1999) criterion yields critical semimajor axes of about 72, 50 and 99 au, for cases (i), (ii) and (iii) respectively. These values predict that the simulations in cases (i) and (ii) would largely become unstable on the main sequence, and those in case (iii) would remain stable during this phase. Such outcomes are largely borne out by the results of the simulations, which we now present.

4 SIMULATION RESULTS

The immediate and over-riding result of our simulations (see Fig. 1) is that 397 out of all 400 simulations eventually become unstable, and do so almost exclusively on the main sequence or during the transition between the giant branch and white dwarf phases. All 200 simulations from cases (i) and (ii) become unstable. In the ‘precarious case’, all systems became unstable on the main sequence, and within 10 Myr, and such that the instability is in the form of ejection. In the ‘nominal case’, 96% of all systems featured ejections, 97% of which occurred on the main sequence. Of the four systems which did not feature ejection, three showcased planet engulfment into HD 131399A and the other engulfment into the approximated star. The engulfments into HD 131399A all occurred after the star became a white dwarf, but within

3 Myr of that phase change. The engulfment into the approximated star occurred within a few Myr of the start of the simulation, and most likely would have resulted in ejection if the binary was resolved (Smullen et al. 2016).

The ‘guarded case’ (case iii) has a more varied set of outcomes, as highlighted in Fig. 1. Of the 197 simulations which became unstable, 70% were in the form of ejections, 28% in the form of engulfment into HD 131399A, and the remainder engulfment into the approximated star. Every ejection occurred after the star became a white dwarf, and within 19 Myr of that moment in all but one case (this case corresponding to a white dwarf “cooling age” of 102 Myr). Alternatively, engulfments into HD 131399A occurred at a variety of times over all phases (right-hand panel of Fig. 1), implying that the qualitative dynamics are highly sensitive to the choice of inclinations, longitudes of ascending node, arguments of pericentre and/or mean anomalies. However, as seen from the bottom-right panel of Fig. 1, clusters of these engulfments occur near the end of the red giant branch and asymptotic giant branch phases of HD 131399A. The one planet which featured engulfment into the approximated star did so 12 Myr after HD 131399A became a white dwarf.

The foundation of the large qualitative dynamical difference between the guarded case and the other two cases is the initial separation between the planet and the approximated star. In the nominal and precarious cases, this separation is almost always small enough to trigger three-body gravitational scattering, and predominately ejection. In the guarded case, the separation is larger, but in most instances not large enough to generate a different outcome. In the other instances, however, the planet experiences secular oscillations in eccentricity and inclination from the approximated star. Eventually the eccentricity becomes high enough to create a collision, especially after HD 131399A’s radius is inflated at the tips of the red giant branch and asymptotic giant branch phases.

These general statements hide the more complex dependencies on each orbital parameter in individual systems. This sensitivity is highlighted by the three stable simulations, which all feature tightly clustered initial inclinations of $i_{\text{pl}} = 103^\circ - 112^\circ$ and $i_{\text{bin}} = 55^\circ - 69^\circ$. Figure 2 presents a schematic of the evolution of one of those simulations on the $y - z$ plane. The outer rim of blue dots indicates that even though the planet is stable during the white dwarf phase of HD 131399A, that stability is fragile.

Our results are consistent with the simulations by Wagner et al. (2016), although the scope and particulars of each set are very different. The most important difference is the duration of the simulations: theirs ran for 100 Myr only on the main sequence. Their chosen orbital parameters would fall somewhere between our nominal and guarded cases, and they imply that all of their simulations remained stable. Stability over 100 Myr on the main sequence is an easy threshold to surpass in our guarded case, but more difficult to achieve in the nominal case (see Fig. 2).

4.1 Caveats

Our results are subject to a number of caveats.

- Ejection is determined at the point where the planet

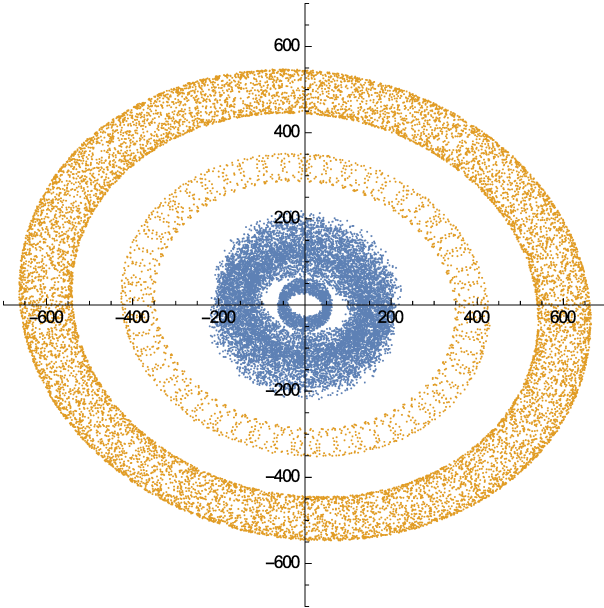


Figure 2. y - z plane schematic in au of one of the only three simulations (out of 400 total) which remained stable for 12.8 Gyr. In this instance, the initial orbital parameters were $a_{\text{pl}} = 55$ au, $e_{\text{pl}} = 0.1$, $i_{\text{pl}} \approx 112^\circ$, $a_{\text{bin}} = 390$ au, $e_{\text{bin}} = 0.1$, and $i_{\text{bin}} \approx 55^\circ$. All simulation outputs are plotted. The blue dots represent the planet (HD 131399Ab) and the orange dots the approximated star which emulates the combination of HD 131399B and HD 131399C at their barycentre. The inner and outer rings for each set of dots indicates evolution along the main sequence and white dwarf phases, respectively. Note the extended dynamic range of the outer ring of blue dots, which is due to a more delicate stability on the white dwarf phase of HD 131399A.

leaves the Hill ellipsoid of the system. As the axes of this ellipsoid have a scale of the order of 10^5 au, a planet may take Myrs to technically be ejected from the system after becoming unbound from HD 131399A. Such variations (of a few Myr) do not affect our overall results.

- Our code does not include tidal effects, which could alter the engulfment statistics. Tides have a much greater reach than the star’s physical radius (by up to a factor of a few) when the star expands onto the red giant branch (Villaver & Livio 2009; Kunitomo et al. 2011; Adams & Bloch 2013; Villaver et al. 2014) and asymptotic giant branch (Mustill & Villaver 2012; Nordhaus & Spiegel 2013; Staff et al. 2016). Hence, if HD 131399Ab was perturbed into an orbit with a high-enough eccentricity such that its pericentre was within a few au of its parent star during one of these phases, its future evolution may be affected. Incorporation of tides into the code is far beyond the scope of this paper, given their complexity, and at most they would cause a marginal change in the instability type percentages.

- Both HD 131399B and HD 131399C are approximated as a single star. This approximation is good enough for our purposes, given that (i) the effects of modelling both stars would have prevented us from simulating the system for over 1 Gyr because of the prohibitive timestep that would be required, and (ii) their differential effect on the planet is negligible (Fig. S3 of Wagner et al. 2016). The consequence is that engulfment into those stars is not correctly modelled,

a case we encountered only a handful of times. Further, in no instance did we see the planet “hop” from HD 131399A to the approximated star (Kratter & Perets 2012); the dynamics of hopping instead to a tight binary might represent an intriguing future project.

5 SUMMARY

We have determined the fate of the planet in the HD 131399 triple star system across all phases of stellar evolution of the A-star planet host, which will become a white dwarf. The computational expense of our long-term (12.8 Gyr) simulations restricted our exploration to three sets of semimajor axes and eccentricities that straddle the error bars of the observations reported in Wagner et al. (2016). We found that the planet becomes unstable in 397 out of 400 realisations. The instability primarily comes in the form of ejection. Whether the ejection occurs on the planet-host’s main sequence phase or during the transition between its giant branch and white dwarf phases depends on the adopted orbital parameters.

The strong evidence for an unstable outcome has pivotal implications for any extant currently-undetected smaller bodies in the system, such as an exo-asteroid belt analogue, exo-Kuiper belt analogue, moons or planets. Instability could trigger excitation of belt constituents – perturbing them into the white dwarf and polluting it, even in the presence of a binary companion (Zuckerman 2014) – either from the single known planet only (Bonsor et al. 2011; Debes et al. 2012; Frewen & Hansen 2014; Antoniadou & Veras 2016) or multiple currently unseen planets (Mustill et al. 2016a), or solely due to the companion star (Bonsor & Veras 2015; Hamers & Portegies Zwart 2016a; Petrovich & Muñoz 2016). Liberated moons (Payne et al. 2016a,b) and multi-planet scattering within a multiple-star system (Veras et al. 2016c) can more generally contribute to active post-main-sequence dynamical environments around systems like HD 131399. Because the current population of metal-polluted white dwarfs largely arose from A-star progenitors such as HD 131399A, that star represents a notable example in the continuing effort to appreciate the full life cycle of planetary systems.

ACKNOWLEDGEMENTS

We thank Adrian Hamers, the referee, for his spot-on suggestions, as well as independently verifying our claim that the binarity of HD 131399B and HD131399C does not affect our calculations. DV and BTG have received funding from the European Research Council under the European Union’s Seventh Framework Programme (FP/2007-2013)/ERC Grant Agreement n. 320964 (WDTracer). AJM is supported by the Knut and Alice Wallenberg Foundation.

REFERENCES

- Adams, F. C., & Bloch, A. M. 2013, *ApJL*, 777, L30
 Antoniadou, K. I., & Veras, D. 2016, *MNRAS*, 463, 4108

- Bergin, E. A., Blake, G. A., Ciesla, F., Hirschmann, M. M., & Li, J. 2015, *Proceedings of the National Academy of Science*, 112, 8965
- Bonsor, A., Mustill, A. J., & Wyatt, M. C. 2011, *MNRAS*, 414, 930
- Bonsor, A., Kennedy, G. M., Wyatt, M. C., Johnson, J. A., & Sibthorpe, B. 2014, *MNRAS*, 437, 3288
- Bonsor, A., & Veras, D. 2015, *MNRAS*, 454, 53
- Bryan, M. L., Knutson, H. A., Howard, A. W., et al. 2016, *ApJ*, 821, 89
- Campante, T. L., Barclay, T., Swift, J. J., et al. 2015, *ApJ*, 799, 170
- Carter-Bond, J. C., O'Brien, D. P., Delgado Mena, E., et al. 2012, *ApJL*, 747, L2
- Chambers, J. E. 1999, *MNRAS*, 304, 793
- Clanton, C., & Gaudi, B. S. 2016a, *ApJ*, 819, 125
- Clanton, C., & Gaudi, B. S. 2016b, Submitted to *AAS Journals*, arXiv:1609.04010
- Debes, J. H., Walsh, K. J., & Stark, C. 2012, *ApJ*, 747, 148
- Dennihy, E., Debes, J. H., Dunlap, B. H., et al. 2016, *ApJ In Press*, arXiv:1608.04384
- Durkan, S., Janson, M., & Carson, J. C. 2016, *ApJ*, 824, 58
- Farihi, J. 2016, *New Astronomy Reviews*, 71, 9
- Forgan, D., Parker, R. J., & Rice, K. 2015, *MNRAS*, 447, 836
- Frewen, S. F. N., & Hansen, B. M. S. 2014, *MNRAS*, 439, 2442
- Gänsicke, B. T., Marsh, T. R., Southworth, J., & Rebassa-Mansergas, A. 2006, *Science*, 314, 1908
- Gänsicke, B. T., Koester, D., Farihi, J., et al. 2012, *MNRAS*, 424, 333
- Gänsicke, B. T., Aungwerojwit, A., Marsh, T. R., et al. 2016, *ApJL*, 818, L7
- Gary, B. L., Rappaport, S., Kaye, T. G., Alonso, R., & Hamsch, F.-J. 2016, Submitted to *MNRAS*, arXiv:1608.00026
- Gill, D. 1897, *Astronomische Nachrichten*, 144, 89
- Gurri, P., Veras, D., Gänsicke, B. T. 2016, *MNRAS In Press*, arXiv:1609.02563
- Hamers, A. S., & Portegies Zwart, S. F. 2016a, *MNRAS*, 462, L84
- Hamers, A. S., & Portegies Zwart, S. F. 2016b, *MNRAS*, 459, 2827
- Hollands, M. et al. 2016, *In Prep*
- Holman, M. J., & Wiegert, P. A. 1999, *AJ*, 117, 621
- Hurley, J. R., Pols, O. R., & Tout, C. A. 2000, *MNRAS*, 315, 543
- Jura, M., & Young, E. D. 2014, *Annual Review of Earth and Planetary Sciences*, 42, 45
- Koester, D., Gänsicke, B. T., & Farihi, J. 2014, *A&A*, 566, A34
- Kostov, V. B., Moore, K., Tamayo, D., Jayawardhana, R., & Rinehart, S. A. 2016, *ApJ In Press*, arXiv:1610.03436
- Kratter, K. M., & Perets, H. B. 2012, *ApJ*, 753, 91
- Kunitomo, M., Ikoma, M., Sato, B., Katsuta, Y., & Ida, S. 2011, *ApJ*, 737, 66
- Lillo-Box, J., Barrado, D., & Correia, A. C. M. 2016, *A&A*, 589, A124
- Luhman, K. L., Burgasser, A. J., & Bochanski, J. J. 2011, *ApJL*, 730, L9
- Manser, C. J., Gänsicke, B. T., Koester, D., Marsh, T. R., & Southworth, J. 2016a, *MNRAS*, 462, 1461
- Manser, C. J., Gänsicke, B. T., Marsh, T. R., et al. 2016b, *MNRAS*, 455, 4467
- Marois, C., Macintosh, B., Barman, T., et al. 2008, *Science*, 322, 1348
- Marois, C., Zuckerman, B., Konopacky, Q. M., Macintosh, B., & Barman, T. 2010, *Nature*, 468, 1080
- Marzari, F., & Gallina, G. 2016, *In Press A&A*, arXiv:1609.05016
- Melis, C., & Dufour, P. 2016, arXiv:1610.08016
- Mordasini, C., van Boekel, R., Mollière, P., Henning, T., & Benneke, B. 2016, *ApJ In Press*, arXiv:1609.03019
- Morlok, A., Mason, A. B., Anand, M., et al. 2014, *Icarus*, 239, 1
- Mustill, A. J., & Villaver, E. 2012, *ApJ*, 761, 121
- Mustill, A. J., Marshall, J. P., Villaver, E., et al. 2013, *MNRAS*, 436, 2515
- Mustill, A. J., Veras, D., & Villaver, E. 2014, *MNRAS*, 437, 1404
- Mustill, A. J., et al. 2016a, *In Prep*
- Mustill, A. J., et al. 2016b, *In Prep*
- Nordhaus, J., & Spiegel, D. S. 2013, *MNRAS*, 432, 500
- Payne, M. J., Veras, D., Holman, M. J., Gänsicke, B. T. 2016a, *MNRAS*, 457, 217
- Payne, M. J., Veras, D., Gänsicke, B. T., Holman, M. J. 2016b, *MNRAS In Press*, arXiv:1610.01597
- Petrovich, C., & Muñoz, D. J. 2016, arXiv:1607.04891, Submitted to *AAS Journals*
- Portegies Zwart, S. 2013, *MNRAS*, 429, L45
- Rappaport, S., Gary, B. L., Kaye, T., et al. 2016, *MNRAS*, 458, 3904
- Ramírez, I., Khanal, S., Aleo, P., et al. 2015, *ApJ*, 808, 13
- Reggiani, M., Meyer, M. R., Chauvin, G., et al. 2016, *A&A*, 586, A147
- Smullen, R. A., Kratter, K. M., & Shannon, A. 2016, *MNRAS*, 461, 1288
- Spina, L., Meléndez, J., & Ramírez, I. 2016, *A&A*, 585, A152
- Staff, J. E., De Marco, O., Wood, P., Galaviz, P., & Passy, J.-C. 2016, *MNRAS*, 458, 832
- Sumi, T., Kamiya, K., Bennett, D. P., et al. 2011, *Nature*, 473, 349
- Smullen, R. A., Kratter, K. M., & Shannon, A. 2016, *MNRAS*, 461, 1288
- Sutherland, A. P., & Fabrycky, D. C. 2016, *ApJ*, 818, 6
- Tremblay, P.-E., Cummings, J., Kalirai, J. S., et al. 2016, *MNRAS*, 461, 2100
- Trifonov, T., Reffert, S., Zechmeister, M., Reiners, A., & Quirrenbach, A. 2015, *A&A*, 582, A54
- Vanderburg, A., Johnson, J. A., Rappaport, S., et al. 2015, *Nature*, 526, 546
- Veras, D., Wyatt, M. C., Mustill, A. J., Bonsor, A., & Eldridge, J. J. 2011, *MNRAS*, 417, 2104
- Veras, D., & Raymond, S. N. 2012, *MNRAS*, 421, L117
- Veras, D., & Tout, C. A. 2012, *MNRAS*, 422, 1648
- Veras, D., Mustill, A. J., Bonsor, A., & Wyatt, M. C. 2013, *MNRAS*, 431, 1686
- Veras, D., & Evans, N. W. 2013, *MNRAS*, 430, 403
- Veras, D., Leinhardt, Z. M., Bonsor, A., Gänsicke, B. T. 2014a, *MNRAS*, 445, 2244
- Veras, D., Evans, N. W., Wyatt, M. C., & Tout, C. A. 2014b, *MNRAS*, 437, 1127

- Veras, D., Shannon, A., Gänsicke, B. T. 2014c, MNRAS, 445, 4175
- Veras, D., Gänsicke, B. T. 2015, MNRAS, 447, 1049
- Veras, D., Leinhardt, Z. M., Eggl, S., Gänsicke, B. T. 2015a, MNRAS, 451, 3453
- Veras, D., Brown, D. J. A., Mustill, A. J., & Pollacco, D. 2015b, MNRAS, 453, 67
- Veras, D. 2016a, Royal Society Open Science, 3, 150571
- Veras, D. 2016b, MNRAS In Press, arXiv:1608.07580
- Veras, D., Carter, P. J., Leinhardt, Z. M., Gänsicke, B. T. 2016a, MNRAS In Press, arXiv:1610.06926
- Veras, D., Mustill, A. J., Gänsicke, B. T., et al. 2016b, MNRAS, 458, 3942
- Veras, D., Georgakarakos, N., Dobbs-Dixon, I., Gänsicke, B. T., et al. 2016c, MNRAS, 458, 3942
- Villaver, E., & Livio, M. 2009, ApJL, 705, L81
- Villaver, E., Livio, M., Mustill, A. J., & Siess, L. 2014, ApJ, 794, 3
- Wagner, K., Apai, D., Kasper, M., et al. 2016, Science, 353, 673
- Wang, L., Kouwenhoven, M. B. N., Zheng, X., Church, R. P., & Davies, M. B. 2015, MNRAS, 449, 3543
- Wilson, D. J., Gänsicke, B. T., Koester, D., et al. 2014, MNRAS, 445, 1878
- Wilson, D. J., Gänsicke, B. T., Koester, D., et al. 2015, MNRAS, 451, 3237
- Wilson, D. J., Gänsicke, B. T., Farihi, J., & Koester, D. 2016, MNRAS, 459, 3282
- Wittenmyer, R. A., Liu, F., Wang, L., et al. 2016, AJ, 152, 19
- Xu, S., Jura, M., Koester, D., Klein, B., & Zuckerman, B. 2014, ApJ, 783, 79
- Xu, S., & Jura, M. 2014, ApJL, 792, L39
- Xu, S., Jura, M., Dufour, P., & Zuckerman, B. 2016, ApJL, 816, L22
- Zuckerman, B., & Becklin, E. E. 1987, Nature, 330, 138
- Zuckerman, B. 2014, ApJL, 791, L27